Proceeding Paper

Towards an Operational Forecast Model Suite for Compound Inundation due to Flash Floods and Storm Tides in Coastal Areas with Non-Perennial Rivers [†]

Angelos Kokkinos [1,*], Christos V. Makris [2], Yannis Androulidakis [4], Zisis Mallios [1], Ioannis Pytharoulis [4], Theofanis Karambas [1] and Yannis Krestenitis [1]

[1] Department of Civil Engineering, Aristotle University of Thessaloniki, 54124 Thessaloniki, Greece; angeloks@civil.auth.gr, zmallios@civil.auth.gr, karambas@civil.auth.gr, ynkrest@civil.auth.gr,

[2] Department of Civil Engineering, Democritus University of Thrace, 67100 Xanthi, Greece; cmakris@civil.duth.gr

[3] Department of Marine Sciences, University of the Aegean, 81100 Mytilene, Greece; iandroul@aegean.gr

[4] Department of Geology, Aristotle University of Thessaloniki, 54124 Thessaloniki, Greece; pyth@geo.auth.gr

* Correspondence: angeloks@civil.auth.gr

† Presented at the 9th International Electronic Conference on Water Sciences, Online, 11-14 November 2025.

Abstract

This study presents a two-dimensional hydraulic modelling framework for the simulation of flash and compound flooding in coastal urban areas with non-perennial river systems. The model employs a rain-on-grid approach within HEC-RAS 2D to simulate rainfall-driven runoff and explicitly incorporates coastal water-level forcing to represent storm tides. The framework is applied to an ungauged coastal basin in northern Greece using a 50-year return period design storm. Model results show good agreement with official Flood Risk Management Plan maps while identifying additional inundated areas linked to lower-order streams. Compound flooding simulations indicate a 21% increase in flooded areas, highlighting the importance of integrated modelling for operational flood forecasting.

Keywords: compound flooding; flood modelling; hydraulic modelling; rain-on-grid; HEC-RAS 2D; operational flood forecasting; coastal zone; storm tide

1. Introduction

In recent years, the frequency of floods has increased due to human interventions in the natural environment and the impacts of climate change. Urbanisation within river floodplains has intensified community exposure to flood risk. Additionally, coastal zones influenced by non-perennial river systems face an elevated risk of flooding due to the combined effects of pluvial events, fluvial overflows, and storm surges, a situation further aggravated by climate change and uncontrolled urbanisation. Particularly hazardous because of their rapid onset are flash floods, which are triggered by intense rainfall over short periods.

To simulate such phenomena, 2D hydrodynamic models are widely used for flood extent mapping because they yield more detailed and reliable results for complex flow simulations. Additionally, 2D models can simulate the timing and duration of inundation with adequate accuracy [1–3]. A further step in these models is the inclusion of spatial

rainfall information via the rain-on-grid (RoG) method [4–6]. In this approach, rainfall is applied directly to each cell of the two-dimensional hydraulic model, thereby simulating surface runoff without requiring an intermediate hydrological model to convert precipitation into runoff. The main advantage of this method is its ability to physically simulate the catchment's hydrological behaviour rather than estimate parameters using conventional hydrological approaches. This is particularly important for simulating flash floods caused by localised storm events (pluvial floods), where overtopping of torrents and tributaries makes deriving hydrographs using hydrological models challenging. On the other hand, a key limitation of the method is the occurrence of shallow flows, which may require adjustments of roughness coefficients, as these may deviate from the standard values commonly used in fluvial flood simulations. In addition, RoG models are single-event simulation models with limited capacity to represent a watershed's hydrological behaviour, requiring additional parameter estimation to estimate effective rainfall. In non-perennial Mediterranean catchments, where flow initiation is dominated by infiltration-excess and rapid surface routing, rain-on-grid formulations offer a physically consistent alternative to hydrograph-based coupling, particularly under operational time constraints.

This study presents a hydraulic model that implements the RoG method to simulate flash floods in a coastal basin with urban fabric. The aim of the model is to forecast flash floods using available meteorological precipitation data, as part of an integrated framework for simulating and forecasting compound flooding in the Thermaikos Gulf, northern Greece [7]. Hence, the focus of the study lies not only on the level of detail and the accuracy of the results, but also on the computational time required for the simulations, which should be as short as possible. Finally, the framework enables the explicit simulation of compound flooding, integrating rainfall-driven flash floods (both fluvial and pluvial components) with coastal water-level forcing from storm surges, tides, and sea-level rise within a unified 2D hydraulic model.

2. Data and methods

2.1 Study Area

The study area consists of the coastal zone east of the Thermaikos Gulf [7], extending from Thessaloniki International Airport to the town of Agia Triada, and includes the urban fabric of Peraia (Figure 1). The study area is classified as a Flood Risk Zone according to the Flood Risk Management Plan (FRMP) of the Central Macedonia Water District [8]. It features a well-developed hydrographic network, with the Livadaki torrent (1st order network in Figure 1) as the main channel, located between the airport and the urban area of Peraia, and a series of second- and third-order streams that run transversely across the entire coastal urban area.

2.2 Data

The digital elevation model (DEM) for the catchment is provided by the National Cadastre of Greece, with a spatial resolution of 2×2 m². The DEM was checked and corrected where necessary, particularly in areas near bridges along the main and the secondary streams. In addition, buildings in urban areas, which are shown in Figure 1, were represented as solid objects, within which flow is excluded. This is achieved by locally increasing the DEM elevation for each building, so that the terrain corresponding to constructed artefacts is particularly higher than the surrounding bare earth. Land-use data obtained from the CORINE Land Cover system, with a spatial resolution of 30×30 m². Figure 1 also shows the land uses of the area, where the CORINE Land Cover classes were merged into a reduced number of land-use categories according to their assigned Manning's roughness values, in order to simplify the parameterisation of surface roughness. These data indicate that the study area is predominantly agricultural, with permanently

irrigated and non-irrigated croplands covering nearly half of the total area (49.7%), fol- 91
lowed by complex cultivation patterns and mixed forest–shrub formations, which to- 92
gether account for 28.2%. Urban land uses, including continuous and discontinuous urban 93
fabric, transport infrastructure, ports, and airport facilities, represent a substantial share 94
(21.4%), reflecting the strong influence of urbanisation. Marine areas occupy a negligible 95
proportion of the study area (0.7%). The Manning's coefficients assigned to each land use 96
category follow the detailed work of [9] on hydraulic modelling of coastal inundation and 97
were set to 0.012, 0.018, 0.040, and 0.140 for continuous urban fabric, discontinuous urban 98
fabric, arable land, and complex cultivation patterns-mixed forests, respectively. 99
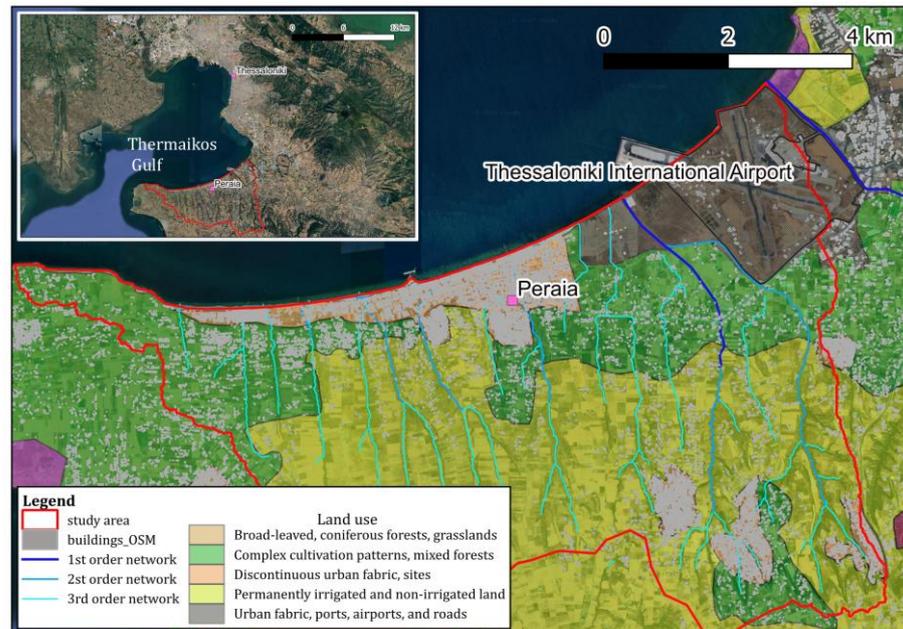
Figure 1. Map of the study area. The map depicts the land-use classes used for the selection of 101
roughness coefficients, as well as the hydrographic network of the area and the buildings in urban 102
and semi-urban areas. 103

The storm event used in this study corresponds to a 50-year return period. To derive 104
the design hyetograph (Figure 2) of the total precipitation, the available intensity–dura- 105
tion–frequency (IDF) curves for the study area were used. The IDF curves have been de- 106
veloped at the national scale within the framework of implementing the EU Floods Di- 107
rective (2007/60/EC). The design storm duration is 48 hours, in accordance with the FRMP 108
for this area. 109

The SCS–CN method [10] was used to estimate effective rainfall from total precipita- 110
tion; it is used exclusively to estimate effective rainfall volumes and does not represent 111
flow routing or storage, which are entirely resolved by the 2D hydraulic solver. This 112
method does not account for soil and groundwater storage; therefore, it is suitable for 113
simulating single-storm events. The effective rainfall is derived from the total rainfall, 114
subtracting the precipitation loss as: 115

$$I = \frac{(P-\lambda S)^2}{(P+S-\lambda P)} \ , \ S = \left(\frac{25400}{CN}\right) - 10 \tag{1}$$

where I is the accumulated precipitation excess in mm, P is the accumulated precipitation 116
depth, λ is the initial abstraction rate equal to 0.2, and S is the maximum soil retention in 117
mm. CN is defined spatially (not shown) based on the CN map developed during the first 118
revision of the area Flood Risk Management Plan of the area [8]. CN values selected refer 119
to normal antecedent moisture conditions (AMC II). Dry-channel conditions were 120

assumed, as there is no baseflow in the streams. Although detailed information on the urban drainage network was not available to explicitly account for its dynamic response, its impact was approximated by assuming a constant minimum infiltration rate of 0.22 mm h⁻¹, applied uniformly across the urban areas.
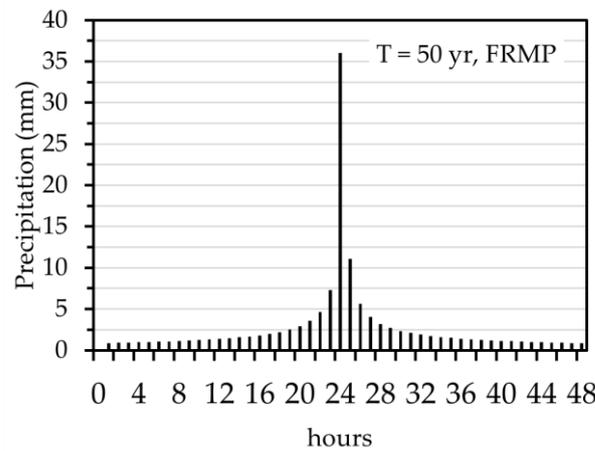
Figure 2. Hourly hyetograph of the simulated design storm scenario that corresponds to a 50-year return period storm.

2.3 Methods

The hydraulic simulations were performed using the HEC-RAS v6.7 model [11], applying both the Diffusive Wave equations (DSW). The computational domain covers the entire study area to account for rainfall over its full extent. Boundary conditions were applied only as outflow conditions at the limits of the computational domain. No inflow conditions were imposed, as rainfall is introduced as a source term in each computational cell. As a downstream boundary condition, when coastal flooding is considered, a uniform total seawater depth was specified along the entire coastline. At this stage, the coastal boundary condition represents a still-water level of 0.98 m, corresponding to the 50-year return level scenario of the updated FRMP [8] (represents a static storm-tide envelope, not dynamic surge propagation). When only precipitation-driven flash flooding is considered, a normal-depth boundary condition is applied at the downstream boundary, with appropriate longitudinal slopes defined locally according to the area's topography.

Since the model is intended to be operational, reducing computational runtime is a key objective, which primarily depends on the size of the computational mesh. For this reason, simulations were performed using grid resolutions of 100 × 100 m², 50 × 50 m², and 25 × 25 m². Local grid refinement was applied along the stream channels and the urban areas using resolutions of 20 × 20 m², 10 × 10 m², and 5 × 5 m², respectively.

3. Results and Discussion

Although the study area is prone to both coastal and flash flooding, it is an ungauged catchment for which no flood events are recorded in remote sensing data. This makes the direct validation of the computational model challenging. The only available reference results for the area are those provided by the FRMP, which show flooding due to precipitation produced through two-dimensional hydrodynamic simulations using design hydrographs for the main watercourses. For coastal inundation, the FRMP's assessment of coastal flood extent used a static 'bathtub' approach with hydraulic connectivity, approximating inundation as areas with ground elevations less than or equal to the estimated sea level rise corresponding to a given return period. Beyond the application of good modelling practices, as described in the EU Floods Directive framework, the reliability of these

flood maps is further enhanced by a formal consultation process with local authorities, professional engineers, and the public, through which local knowledge and experience were incorporated. Consequently, comparing our model results with the FRMP flood maps ensures that the developed model achieves an accuracy comparable to that used in official governmental flood risk management actions.

Figure 3 presents the flood-extent map from the FRMP for the study area, based on a 50-year return-period design hydrograph for the Livadaki stream. The figure also shows the flood extent for the same storm event obtained with the RoG model at a 25 × 25 m² mesh resolution, considering only fluvial/pluvial flooding. The comparison indicates that the flood extent simulated by the RoG model is larger than that depicted in the FRMP maps. This difference is attributed to the distinct representation of surface runoff in the two modelling approaches, highlighting the advantage of the RoG method in areas characterised by numerous small streams. The additional inundated areas identified by the RoG simulation originate primarily from spatially distributed runoff generation and the activation of second- and third-order channels, which are not explicitly represented in hydrograph-based FRMP modelling. This highlights the importance of spatial rainfall representation in urbanised coastal basins with dense ephemeral drainage networks. The RoG model successfully captures the entire flooded area identified in the FRMP maps, achieving a hit rate of 92%, while also identifying areas flooded by lower-order streams or by direct rainfall accumulation (i.e., interpreted as pluvial-dominated flooding rather than overestimation). A representative example is the airport area, where the largest discrepancy between the two flood maps is observed. The FRMP map depicts a smaller flooded extent originating exclusively from the Livadaki stream, whereas the RoG model indicates more extensive flooding due to rainfall occurring directly over the airport area. Although the airport has been treated as an urban area with extensive impervious surfaces, information on its surface drainage system is classified; therefore, the model results for this area cannot be considered fully accurate.
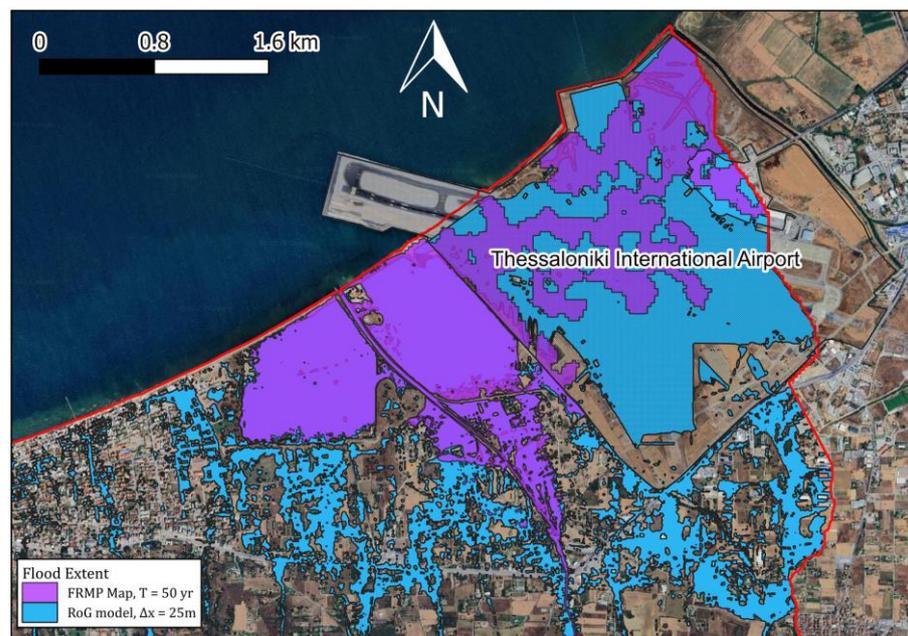
Figure 3. Fluvial/Pluvial flood extent comparison for a 50-year return period event from the FRMP vs. the RoG model (25 × 25 m² mesh).

Figure 4 shows the comparison between the coastal flood extent estimated within the framework of the FRMPs and the extent computed by the present simulations at a grid resolution of Δx = 5 m in the coastal area. The simulated inundation extent is largely

consistent with that of the FRMPs, both in the area around the Livadaki stream and in the 190
urban area of Peraia (Figure 4 inset map). It should be noted, however, that the FRMP- 191
derived flood extents inherently reflect structural uncertainties associated with the under- 192
lying methodological assumptions, such as hydrograph-based routing schemes and sim- 193
plified "bathtub" approaches for coastal inundation. Consequently, the comparison pre- 194
sented herein should be interpreted as a comparison between two distinct modelling 195
frameworks rather than a validation against observations. The inundated area derived 196
from the simulations is more limited than that of the FRMPs, which is attributed to both 197
the inclusion of buildings in the simulations and, more importantly, to the more detailed 198
computational approach adopted, which renders the results more reliable. 199

200
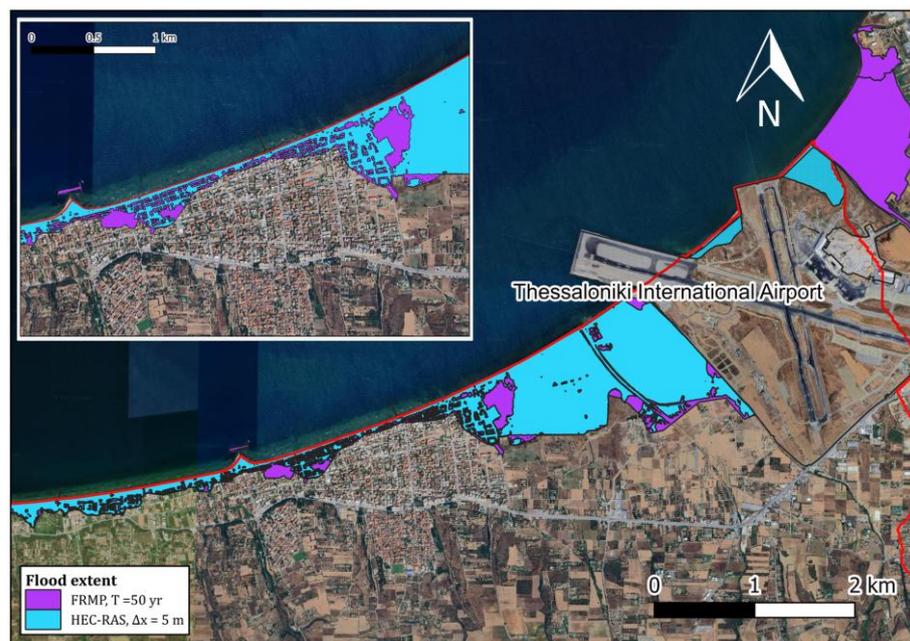
Figure 4. Coastal flood extent comparison for a 50-year return period event from the FRMP vs. the 201
HEC-RAS model (5 × 5 m² mesh). 202

Finally, Figure 5 compares the maximum flood extent maps from the rainfall-only 203
and compound flooding scenarios to assess the contribution of each flooding source to the 204
final inundation. In this simulation, a 10 m grid is used in the urban areas and the stream 205
channels, and a 50 m grid for the rest of the area. The results indicate that the additional 206
flooded area resulting from the inclusion of storm surge/tide amounts to 21% and is ob- 207
served not only along the coastal waterfront but also within the urban interior. 208

Although detailed information, such as flood depth and velocity, is particularly val- 209
uable for the design of risk management measures, this study focuses on evaluating the 210
flood extent map, which is often sufficient for operational modelling purposes when avail- 211
able in a timely manner. Comparing the flood extent map of the examined grid resolutions 212
for flood due to precipitation, it is found that the model employing a 25 × 25 m² mesh 213
produces the largest flood extent, while simulations with 50 × 50 m² and 100 × 100 m² 214
meshes reproduce 93% and 88% of this extent, respectively. For these simulations, the ra- 215
tio T_{sim}/T_{com} equals 27.6, 22.6, and 5.95 for grid resolutions of 25 × 25 m², 50 × 50 m², and 216
100 × 100 m², respectively, where T_{sim} denotes the simulation scenario duration (48 hours) 217
and T_{com} the actual computational time. All simulations were performed on an AMD 218
Ryzen 9 7950X 16-Core Processor (4.50 GHz), utilising all cores permitted by the HEC- 219
RAS architecture (8 cores). For a simulation to be considered suitable for operational use, 220
the ratio should be less than 6, thereby allowing timely intervention. Under the given 221

hardware configuration, even the simulation with a 25 × 25 m² mesh marginally satisfies 222
this constraint. For coastal flooding, the grid sensitivity analysis showed practically no 223
difference in flood extent across grid resolutions in the coastal area from 20 m down to 5 224
m, while the T_{sim}/T_{com} was consistently much greater than 6 across all simulations. This 225
aligns with pragmatic guidelines of civil protection agencies about imperative lead times 226
or forecasting update cycles. Therefore, a mesh spacing of 10 m in urban areas and stream 227
channels, and 50 m elsewhere, is a suitable compromise between accuracy and runtime 228
effectiveness for operational modelling with a forecast scope. 229

230

Figure 5. Comparison of the flood extent map between the compound flooding and the precipita- 231
tion-only scenarios. 232

4. Conclusions 233

This study presents a two-dimensional hydraulic modelling framework based on the 234
rain-on-grid approach for simulating flash and compound flooding in a coastal urban ba- 235
sin with non-perennial rivers. The model integrates rainfall-driven runoff with coastal 236
water-level forcing within a unified HEC-RAS 2D environment, aiming to support oper- 237
ational flood forecasting. 238

The results show good agreement with the Flood Risk Management Plan flood ex- 239
tents for precipitation-driven flooding, while identifying additional inundated areas as- 240
sociated with lower-order streams and direct rainfall accumulation. Coastal flooding sim- 241
ulations are largely consistent with official maps but yield more confined inundation due 242
to the inclusion of buildings and the use of a fully hydraulic approach instead of a static 243
bathtub method. The compound flooding scenario indicates a 21% increase in inundated 244
areas compared to rainfall-only conditions, affecting both coastal and inland urban zones. 245

Grid sensitivity analysis indicates that a mixed-resolution mesh, combining fine res- 246
olution in urban areas and stream channels with coarser resolution elsewhere, provides 247
an effective balance between accuracy and computational efficiency, making the proposed 248
framework suitable for operational flood modelling. 249

250

Author Contributions: Conceptualization, A.K., C.M., Y.K. and T.K.; methodology A.K., C.M. and 251
Z.M.; software, A.K. and C.M.; validation, A.K., Z.M. and C.M; formal analysis, A.K., C.M. and Y.A.; 252
investigation, A.K., C.M., Y.A. and Z.M.; resources, A.K., C.M., Z.M. and Y.P.; data curation, A.K., 253
C.M., Y.A., Z.M. and Y.P.; writing—original draft preparation, A.K. and C.M; writing—review and 254

Institutional Review Board Statement: Not applicable.

Informed Consent Statement: Not applicable.

Data Availability Statement: Data are available upon request as they are part of an ongoing research project.

Conflicts of Interest: The authors declare no conflicts of interest.

References

1. Morsy, M.M.; Goodall, J.L.; O'Neil, G.L.; Sadler, J.M.; Voce, D.; Hassan, G.; Huxley, C. A Cloud-Based Flood Warning System for Forecasting Impacts to Transportation Infrastructure Systems. *Environmental Modelling & Software* **2018**, *107*, 231–244, doi:10.1016/J.ENVSOFT.2018.05.007.

2. Ongdas, N.; Akiyanova, F.; Karakulov, Y.; Muratbayeva, A.; Zinabdin, N.; Ongdas, N.; Akiyanova, F.; Karakulov, Y.; Muratbayeva, A.; Zinabdin, N. Application of HEC-RAS (2D) for Flood Hazard Maps Generation for Yesil (Ishim) River in Kazakhstan. *Water 2020, Vol. 12,* **2020**, *12*, 1–20, doi:10.3390/W12102672.

3. Shustikova, I.; Domeneghetti, A.; Neal, J.C.; Bates, P.; Castellarin, A. Comparing 2D Capabilities of HEC-RAS and LISFLOOD-FP on Complex Topography. *Hydrological Sciences Journal* **2019**, *64*, 1769–1782, doi:10.1080/02626667.2019.1671982.

4. David, A.; Schmalz, B.; David, A.; Schmalz, B. A Systematic Analysis of the Interaction between Rain-on-Grid-Simulations and Spatial Resolution in 2D Hydrodynamic Modeling. *Water 2021, Vol. 13,* **2021**, *13*, doi:10.3390/W13172346.

5. Ennouini, W.; Fenocchi, A.; Petaccia, G.; Persi, E.; Sibilla, S. A Complete Methodology to Assess Hydraulic Risk in Small Ungauged Catchments Based on HEC-RAS 2D Rain-On-Grid Simulations. *Natural Hazards* **2024**, *120*, 7381–7409, doi:10.1007/s11069-024-06515-2.

6. Godara, N.; Bruland, O.; Alfredsen, K. Simulation of Flash Flood Peaks in a Small and Steep Catchment Using Rain-on-Grid Technique. *J. Flood Risk Manag.* **2023**, *16*, e12898, doi:10.1111/jfr3.12898.

7. Androulidakis, Y.; Makris, C.; Kolovoyiannis, V.; Kombiadou, K.; Krestenitis, Y.; Kartsios, S.; Pytharoulis, I.; Baltikas, V.; Mallios, Z. Operational Platform for Metocean Forecasts in Thermaikos Gulf (Aegean Sea, Greece). *Journal of Operational Oceanography* **2025**, *18*, 123–149, doi:10.1080/1755876X.2025.2503569.

8. General Secretariat for the Natural Environment and Water, G.D. for W. *1st Revision of the Flood Risk Management Plan for the River Basin District of Central Macedonia (EL10)*; Athens, 2025;

9. Makris, C.; Mallios, Z.; Androulidakis, Y.; Krestenitis, Y.; Makris, C.; Mallios, Z.; Androulidakis, Y.; Krestenitis, Y. CoastFLOOD: A High-Resolution Model for the Simulation of Coastal Inundation Due to Storm Surges. *Hydrology 2023, Vol. 10,* **2023**, *10*, doi:10.3390/HYDROLOGY10050103.

10. Cronshey, R. *Urban Hydrology for Small Watersheds*; US Department of Agriculture, Soil Conservation Service, Engineering Division, 1986;

11. USACE *HEC-RAS Hydraulic Reference Manual Version 6.6*; 2024;